Universiteit
Leiden
The Netherlands

Tracking helminths : from molecular diagnostics to mechanisms behind immune polarization

Kaisar, M.M.

Citation
Kaisar, M. M. (2017, September 19). *Tracking helminths : from molecular diagnostics to mechanisms behind immune polarization*. Retrieved from https://hdl.handle.net/1887/57928

Version:	Not Applicable (or Unknown)
License:	Licence agreement concerning inclusion of doctoral thesis in the Institutional Repository of the University of Leiden
Downloaded from:	https://hdl.handle.net/1887/57928

Note: To cite this publication please use the final published version (if applicable).

Cover Page

Universiteit Leiden

The handle http://hdl.handle.net/1887/57928 holds various files of this Leiden University dissertation

Author: Kaisar, M.M.
Title: Tracking helminths : from molecular diagnostics to mechanisms behind immune polarization
Issue Date: 2017-09-19

Chapter 4

The *Schistosoma mansoni* Lipidome: leads for immunomodulation

MARTIN GIERA[1], MARIA M. M. KAISAR[2, 3], RICO DERKS[1], EVELYNE STEENVOORDEN[1], YVONNE C. M. KRUIZE[2], CORNELIS H. HOKKE[2], MARIA YAZDANBAKHSH[2], BART EVERTS[2]

[1]Center of Proteomics and Metabolomics, LUMC, Leiden, The Netherlands
[2]Department of Parasitology, Leiden University Medical Center (LUMC), Leiden, The Netherlands
[3]Department of Parasitology, Faculty of Medicine, Universitas Indonesia, Jakarta, Indonesia

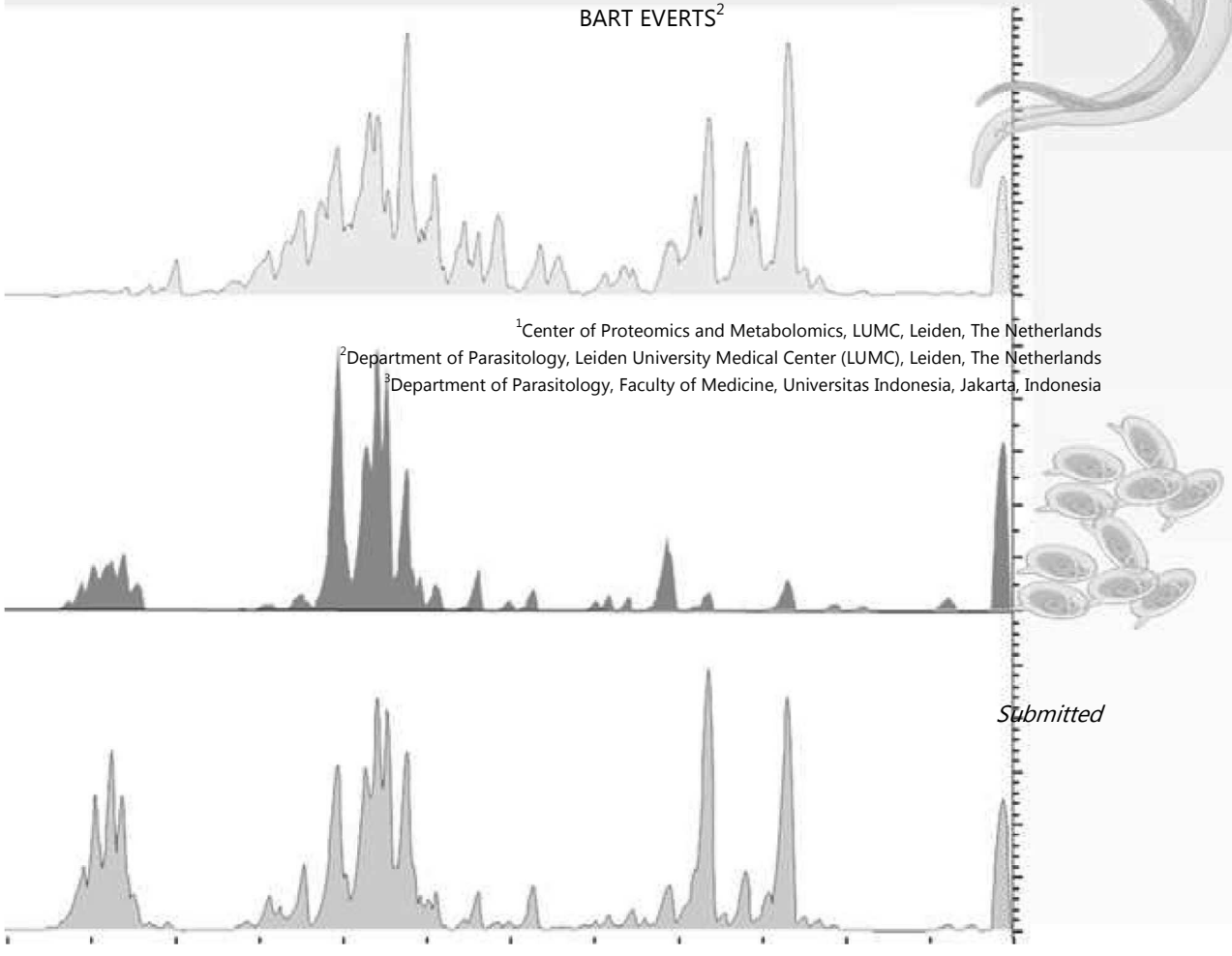

Submitted

ABSTRACT

Schistosoma mansoni is a parasitic helminth that infects millions of people mostly in tropical parts of the world. Different life cycle stages of *S. mansoni,* that infect or develop in the human host, promote distinct immune responses and are known for their ability to modulate host immune responses. However, the molecular mechanisms through which the parasites interact with, and modulate the host immune system remain incompletely understood. Despite the well-known ability of various lipids to modulate immune responses, a comprehensive analysis of the lipidome of the different life cycle stages has not been performed. Using three complementary MS-based platforms to detect and quantify around 400 lipid species, we here characterized the lipid profiles of *S. mansoni* cercariae, worms and eggs, as well as extracts and excretory/secretory (ES) products of different life cycle stages of *S. mansoni*. We identified life cycle stage specific signatures of lipid classes of which cercariae were found to have the most distinct profile. Moreover, we detected several immunolomodulatory oxylipids in the different life cycle stages. Specifically, prostaglandins were found to be most highly enriched in egg preparations, while resolvins were specifically detected in cercariae. Together, the generation of this detailed lipid database of the different life cycle stages of *S. mansoni* will not only be important for a better understanding of the biology of the parasite itself but also of host-parasite interactions and how that could result in immunomodulation.

Keyword:
Schistosoma mansoni, Lipidomics, Excretory/Secretory products, life cycle stages, immunomodulation

INTRODUCTION

Schistosoma mansoni is a parasitic trematode causing schistosomiasis in humans and occurs in mostly tropical parts of South America and Africa. According to the WHO more than 61 million people have been treated for this disease in 2014 [1] with estimates of between 20000 to 200000 deaths per year. The life cycle of this parasite is complex and involves both humans as a final host as well as freshwater snails as intermediate host. Infection of humans is initiated by the larval stage of these parasites, termed cercariae, through their ability to penetrate human skin. Upon penetration cercariae lose their tail, allowing their head to develop into schistosomula that migrate through the skin into the circulation. Two to 3 weeks after the initial infection, schistosomula end up in the hepatoportal circulation where they develop into sexually mature adults and pair for sexual reproduction. Subsequently, approximately 6 to 8 weeks into the infection, females start to produce eggs, of which around 50% through the wall of the intestine to reach the outside environment. However, a large fraction of the eggs get lodged in the intestinal wall or are instead carried by the blood flow into the liver, where they become trapped in hepatic sinusoids. This accumulation of eggs in tissues is the major cause of pathology in schistosomiasis [2].

The immune responses associated with this infection are equally complex. Infection with cercariae initially trigger an immune reaction characterized by a T helper 1 (Th1) response. However, upon egg production, a strong Th2 response is induced that subsequently orchestrates the development of granulomatous lesions surrounding the eggs. *S. mansoni* infections are often chronic in nature, which in part is thought to be due to the ability of these pasasites to promote regulatory responses that dampen type 2 inflammation that can lead to responses against their parasites [3, 4]. Importantly, evidence is accumulating that this induction of regulatory immune responses by *S. mansoni*, may not only impair effector responses directed against the parasite, but may also be beneficial to the host as it can concomitantly lead to bystander suppression of other inflammatory immune responses. For instance, population studies have revealed that these parasitic infections, can reduce various parameters associated with allergic responses [5, 6]. These observations have been corroborated in animal models [7, 8] and further extended to models of other inflammatory disorders including colitis [9] and type 2 diabetes [10]. This illustrates that different life cycle stages of *S. mansoni* that infect or develop in the human host, promote distinct immune responses, that are not only important in mediating immunity against the infection and in determining the immunopathological outcome of the disease, but that can also have beneficial effects on development of various unrelated inflammatory disorders. Therefore, it will be important to define the components and antigens from the different life cycle stages that may drive these distinct immune responses in humans. This could be of great value for vaccine development against *S. mansoni*, but could also contribute to the design of therapeutics to treat inflammatory diseases by exploiting the immunoregulatory potential of some helminth-derived molecules. Thus far, to identify *S. mansoni*-derived molecules with immunomodulatory potential, most studies have focused on proteomics [11, 12] or glycomics [13, 14]. Much less is known about *S. mansoni*-derived lipids in this context.

Already in the late 1960s studies were undertaken to characterize the major lipid classes present in *S. mansoni* worms [15]. Subsequent studies revealed that apart from being constituents of membranes, lipid metabolism in *S. mansoni* also has important roles in development of the different life cycle stages [16] and in evasion of immune responses by adult worms [17] or cercariae [18]. The potential role of lipids interacting with immune system comes from study that has directly linked *S. mansoni* Lyso-PS, to immunomodulation by induction of regulatory T cells [19]. Moreover, there is some evidence to suggest that *S. mansoni* can produce eicosanoids [20],

which are bioactive lipids well recognized for their immunomodulatory capacity. With these studies in mind, it is important to first conduct a comprehensive in-depth characterization of the lipid composition of the different classes of lipids of the distinct life cycle stages of *S. mansoni*. Studies that have performed lipid profiling of *S. mansoni* so far, were either based on a limited fingerprinting approach leading to the identification of a very small number of lipids [21-23] or focused specifically on the phospholipid content of only the worm itself [23, 24]. Using three complementary highly sensitive MS-based lipidomics platforms, we present a comprehensive lipidomics analysis of *S. mansoni* cercariae, adult worm and eggs, as well as of typical extracts of cercariae (cercarial antigen, CA), worms (adult worm antigen, AWA) and eggs of (soluble egg antigen, SEA) and their excretory and secretory products (ES), each widely used in immunological studies. We identified life cycle stage specific lipid signatures not only for membrane and storage lipids but in particular for bioactive lipid mediators, which provides potentially interesting new leads to study the link between the *S. mansoni* lipidome and immunomodulation.

MATERIALS AND METHODS

Chemicals

For all lipids the LipidMaps abbreviation system is used [25]. Oxylipid standards were from Cayman Chemicals (Ann Arbor, MI, USA), the internal standard solution for oxylipid analysis (oxIS) contained each of PGE2-d4, LTB4-d4, 15-HETE-d8 and DHA-d5 at a concentration of 50 ng/mL in methanol (MeOH). The internal standard for lipidomics analysis (lipIS) contained lysophosphatidylcholine LPC (19:0), phosphatidylcholine PC (11:0/11:0), phosphatidylethanolamine PE (15:0/15:0) (Avanti Polar Lipids, Alabaster, AL, USA) and triacylglyceride TG (15:0/15:0/15:0) (Sigma Aldrich) at a concentration of 0.5 µg/mL in 2-propanol. For GC-MS analysis the GLC-85 mix from Nu-check Prep (Elysian, MN, USA) in combination with the volatile acids mix from Sigma Aldrich was used for constructing calibration lines and as authentic standards for substance identification. Palmitic acid d31 1 µg/mL in ethanol was used as internal standard for GC-MS analysis (gcIS) (Cambridge isotopes, Cambridge, MA, USA). All other chemicals were from Sigma-Aldrich (St. Louis, MO, USA). All solvents were of *pro analysi* or LC-MS grade.

Animal and parasite materials

The full life cycle of the Puerto Rican strain of *S. mansoni* used in this study was maintained in *Biomphalaria glabrata* as snail intermediate host and male Golden hamsters (RjHan : AURA, Javier labs) as mammalian definitive host. For infections, male hamsters 9.5 weeks old and weighing ±100 g were exposed to an aqueous suspension containing 1200 cercariae of *S. mansoni* freshly shed by *B. glabrata* infected hamsters were maintained in a controlled environment at room temperature (RT) with normal night and daylight cycle. All hamster experiments were performed in accordance with local government regulations, and the EU Directive 2010/63EU and Recommendation 2007/526/EC regarding the protection of animals used for experimental and other scientific purposes and approved by the CCD. Preparation of parasite samples for lipidomics analysis is described below. For each sample three biological replicates were generated to account for possible parasite batch variations.

Cercariae. *S. mansoni*-infected *B. glabrata* snails kept in trays were transferred to a cup containing 30 mL of mineral water, and exposed to light at 28 °C for 2 h to trigger cercariae shedding. Cercariae were sedimented by cooling on ice, and stored in water at -80 °C until use. Alternatively, as described below, live cercariae were cultured to produce cercarial ES products.

Eggs. Eggs were obtained as described before (Dalton *et al*. 1997), with some modification. Briefly, the livers of 10 hamsters that were infected with *S. mansoni* 6 week before, were homogenised in 300 mL of wash buffer (1.7% NaCl PBS, to prevent hatching of eggs). The suspension was poured into a one-liter screw cap bottle containing 800 mL wash buffer, collagenase B (400 mg), streptomycin and penicillin (750 µl 200.000 U/ml, each) gently stirred at 37 °C overnight. Then the suspension was sequentially sieved through 355 and 200 micron sieves rinsed with wash buffer, and transferred to 50 mL tubes. After centrifugation for 5 min at 400 g, RT the pellets were collected, resuspended in wash buffer, transferred to new 50 mL tubes followed by centrifugation as above. These steps were repeated until the supernatant became clear, with intermediate application to an 80 micron sieve. The isolated eggs were resuspended in wash buffer containing EGTA and EDTA to inactivate collagenase, washed three times with this buffer at 60 g for 3 min, RT. The eggs were collected and counted prior to final wash with wash buffer at 1000 rpm, for 1 min, RT. Aliquots of approximately 50.000 eggs were stored at -80 °C in PBS until use. In addition, live eggs were cultured to generate egg ES, as described below.

Adult worms. Mixed male and female adult worms were obtained from hamsters sacrificed 6 weeks after infection with *S. mansoni*, through perfusion of the hepatic portal system and mesenteric veins. Collected live worms were washed with perfusion buffer (Dulbecco's buffered saline and sodium citrate) to remove blood and debris. Worms were then washed with PBS and stored at -80 °C until use, or cultured to collect worm ES as described in following section.

Preparation of extracts and ES products of *S. mansoni*: cercariae, worms and eggs

Parasite extracts

Cercarial Antigen (CA) and *Soluble Eggs Antigen (SEA)*. Frozen cercariae or eggs were thawed and manually homogenized in a sterilized glass homogenizer on ice. Homogenates were subsequently subjected to sonification (six rounds of 30 sec, with 20 sec intervals) (Branson sonifier) on ice. The extracts were kept overnight at -80 °C. Following thawing extracts were centrifuged twice cat 13000 rpm, 4 °C for 25 min. The supernatants were collected and filter-sterilized. Protein concentration was determined using BCA (Pierce BCA Protein assay kit, Thermo Scientific) according to the manufacturer's protocol. The protein concentrations of CA and SEA were adjusted to 80 µg/ml and samples were stored at -80 °C until use.

Adult Worm Antigen (AWA). Worms were lyophilized, suspended in cold PBS and manually homogenized in a sterilized glass homogenizer. The process was continued as for CA and SEA preparation.

Excretory/secretory (ES) products

Cercarial ES (CES). Approximately 100.000 freshly shed cercariae were suspended in 12.5 mL of M199 medium (Gibco) supplemented with HEPES, antimycotic and L-glutamine (Sigma-Aldrich). The cercariae were incubated for 20 min at 37 °C 5% CO_2, during this period they transform into schistosomula, after which the process continued with centrifugation at 1600 rpm, RT, 5 min, and then the supernatant (CES) was collected.

Egg ES (EES). Approximately 300.000 freshly isolated eggs were resuspended in 25 mL 20% percoll and centrifuged at 500 g for 6 min. The eggs were centrifuged for 4 min, at 1100 rpm, RT for four times: two times with 2 mL PBS (1.7% NaCl); one time with RPMI (Gibco) supplemented with penicillin and streptomycin; and one time with up to 40 mL of medium (RPMI supplemented with fungizone, penicillin and streptomycin—referred as E-medium). The eggs were resuspended in 1

mL of E-medium in 24 well plates and incubated for 48 h at 37 °C 5% CO_2. About 800 µL supernatant was collected (EES).

Worm ES (WES). Live worms were gently washed twice with S-medium (M199 medium (Gibco) supplemented with ABAM (Sigma) and HEPES—referred as S-medium). In total, approximately 200 mixed male and female worms were resuspended in 20 mL of S-medium and placed in a 75cm^3 flask. The flask was incubated at 37 °C 5% CO_2 for 48 h and the supernatant (WES) was collected.

All ES products were kept at -80 °C until further use. Prior to lipidomics analysis, ES preparation concentrations were adjusted to 80 µg/ml. For protein concentration determination by BCA, the medium used for culturing the cercariae, eggs and worms was taken as background.

Sample preparation

Three different types of samples were investigated in this study: 1) whole parasite life cycle stages (cercariae, worms and eggs); 2) water soluble extracts including: CA, AWA, SEA; and 3) ES products (CES, EES and WES). Whole parasite life cycle stages were extracted using 2-propanol after homogenization in a bullet blender for further analysis using mass-spectrometry . In the case of extracts or ES products, 20 µL of sample was directly used for the below described procedures. Briefly, to the parasite materials sample in 150 µL phosphate buffered saline was added 5 stainless steel beads and the sample homogenized for 5 min in a bullet blender. Subsequently 300 µL 2-propanol was added, the sample was vigorously shaken and centrifuged at 16100 ×*g* for 5 minutes. The supernatant was transferred to a glass vial. The residual sample was re-extracted using 300 µL of 2-propanol and the organic extracts combined. The combined organic extracts were dried under a gentle stream of nitrogen and dissolved in 200 µL 2-propanol, stored at -80 °C until analysis.

GC-MS analysis for total fatty acid analysis

GC-MS analysis was carried out as described elsewhere [1, 26], with some modifications. Briefly, to 20 µL sample in a glass vial was added 10 µL of 10 M NaOH and 250 µL acetone. The vial was flushed with nitrogen, tightly closed and incubated at 60 °C for one hour. After cooling to room temperature 10 µL of gcIS solution, followed by the addition of 100 µL of a 172 mM solution of PFBBr in acetone. The samples were subsequently incubated for 30 min at 60 °C. 250 µL of water and 500 µL of n-hexane was added and the hexane layer transferred to an auto sampler vial. GC-ECNI-MS analysis was carried out on a Bruker scion TQ (Bruker, Bremen, Germany) using methane (99.9995%) as CI gas, equipped with an Agilent VF-5MS (30 m × 0.25 mm × 0.25 mm) column. The temperature program was as follows: 1 min 50 °C, linear increase at 40 °C/min to 60 °C, held 3 min at 60 °C, linear increase at 25 °C/min to 237 °C, linear increase at 3 °C/min to 250 °C, linear increase at 25 °C/min to 315 °C held for 1.55 min. The transfer line and ionization source temperature were 280 °C. The pressure of the chemical ionization gas was set at 15 psi. The carrier gas was helium (99.9990%) at a flow rate of 1.2 mL/min.

LC-MS/MS analysis of eicosanoids and docosanoids

Eicosanoid and docosanoid analysis was carried out as described elsewhere [27]. For liquid samples 20 µL sample was mixed with 60 µL MeOH and 2 µL oxIS solution, the sample was centrifuged for 10 min at 16100 ×*g* and 4 °C. 50 µL of the supernatant was dried under a gentle stream of nitrogen and re-dissolved in 50 µL 40% MeOH for injection. Targeted lipidomics analysis was carried out as follows: analysis was achieved using a QTrap 6500 mass spectrometer in

negative ESI mode (ESI-) (Sciex, Nieuwerkerk aan den Ijssel, The Netherlands), coupled to a LC system employing two LC-30AD pumps, a SIL-30AC autosampler, and a CTO-20AC column oven (Shimadzu, 's-Hertogenbosch, The Netherlands). The employed column was a Kinetex C18 50 × 2.1 mm, 1.7 µm, protected with a C8 precolumn (Phenomenex, Utrecht, The Netherlands), kept at 50 °C. The following binary gradient of water (A) and MeOH (B) with 0.01% acetic acid was used: 0 min 30% B, held for 1 min, then ramped to 45% at 1.1 min, to 53.5% at 2 min, to 55.5% at 4 min, to 90% at 7 min, and to 100% B at 7.1 min, held for 1.9 min. The injection volume was 40 µL and the flow rate 400 µL/min. The MS was operated under the same conditions as in reference [28]. For quantification calibration lines, constructed with standard material were used and only peaks with a signal to noise (S/N) > 10 were quantified. For analytes where no calibration line was used, area ratios were used and a S/N > 3 was used as a detection limit. A list of all monitored oxylipids, corresponding lipidmaps IDs and calibration ranges can be found in supplementary (Table S1).

LC-MS analysis for lipid profiling

LC-MS/MS based lipid profiling was carried out as described elsewhere [29, 30] with some modifications. Briefly, a Dionex Ultimate 3000 (Thermo, Oberschleiβheim, Germany) delivered a gradient of water:acetonitrile 80:20 (eluent A) and water:acetonitrile:2-propanol 1:90:9, both containing 5 mM ammonium formate and 0.05% formic acid. The applied gradient was as follows: 0 min 40% B, 10 min 100% B, 12 min 100% B. The flow rate was set to 250 µL/min at a column temperature of 50 °C. The column used was a Phenomenex Kinetex C18, 2.7 µm, 50×2.1 mm (Phenomenex, Utrecht, The Netherlands). The MS was a Bruker Maxis Impact HD, operated in the positive ESI mode (ESI+), with the following conditions: capillary 3500 V, dry gas (nitrogen 99.9990%) 7 L/min, dry temperature 300 °C, nebulizer 2.1 bar, mass range m/z 150-1000. The injection volume was 20 µL.

Lipid identification

For targeted lipidomics employing GC-ECNI-MS and LC-MS/MS (QTrap) analysis, lipids were identified by comparing relative retention times (RRT) and either molecular ions [M]- monitored in selected ion monitoring mode for GC-ECNI-MS analysis or characteristic MRM transitions in case of LC-MS/MS (QTrap) analysis. In case of LC-MS based lipid profiling we made use of the following approach. Initially all MS and MS/MS spectra were recalibrated using the signal of a calibration solution consisting of sodium formate in 50:50 isopropanol:water. The calibration solution was post column injected into the LC effluent in order to elute before the dead time of every analysis. The recalibration was done in Data Analysis 4.2 build 395 (Bruker Daltonik GmbH, Germany). Subsequently, MS/MS acquisition was achieved using a data independent method. Analysis was done per sample per lipid class. For each lipid class characteristic parameters (i.e. retention time range, unique product ion or neutral lost) where set to filter the MS/MS spectra as shown in Table 1.

Within Data Analysis homemade Visual Basic scripts were used to filter all collected MS/MS spectra according to each lipid class separately. The results were exported to mgf format, resulting in a single mgf file per sample per lipid class. Each mgf file was used to search the LipidBlast databases [31]. LipidBlast contains several different libraries, some contain multiple lipid classes others are specific for one lipid class. The top results of all database searches were stored and further processed in R (CRAN R, version 3.3.2). For each sample type three biological sample replicates were measured and only lipids detected in at least two out of three samples were

deposited in our *S. mansoni* lipid database (supplementary Table S2). For calculating percentage (%) lipid composition of all samples we used the MS signals as follows: from the MS/MS data *m/z* and retention time for each lipid were extracted. Subsequently a homemade Visual Basic script was used to automate the following steps within data analysis: create extracted ion chromatogram (EIC) from the *m/z* with a narrow window of 5 mDa, set retention time window around the retention time and finally carry out peak detection and integration. Results of each sample were exported to a comma separated (csv) file. All result files were collected and further processed in R.

Table 1. Lipid class characteristics used for assignment

Lipid class	Retention time range [min]	Product ion	Neutral loss	Precursor
Phosphatidic Acid (PA)			97.9769	
Lyso-Phosphatidic Acid (LPA)		155.06638		
Lyso-Phosphatidylcholine (LPC)		184.0733		Even
Lyso-Phosphatidylethanolamine (LPE)	6.5 – 9.0		141.0191	
Phosphoglycerol (PG)			172.0137	
Phosphoinositol (PI)			260.0297	
Phosphatidylserine (PS)			185.0089	
Sphingomyelins (SM)		184.0733		Odd
Cholesteryl Ester (CE)	10.0 – 12.0	369.3516		Even
Diacylglycerol (DG)	7.0 – 9.5			Even
Triacylglycerol (TG)	10.0 – 12.0			Even

RESULTS

Analysis and identification of lipid species

Using three lipidomics platforms, which were: QToF based LC-MS/MS for major lipid classes, GC-MS for total fatty acid (FA) analysis as well as QTrap based LC-MS/MS for eicosanoid and docosanoid analysis and we investigated occurrence and quantity of several lipid classes in different life-cycle stages of *S. mansoni* that could be of relevance to interaction with human host. The investigated lipid classes, the employed platform and the number of detected species are given in Table 2.

Table 2. Analytical platforms and number of detected lipid species

Analytical Platform	Monitored Lipid Classes	Number of detected Species
GC-MS	Total FA	28
LC-MS/MS (QTrap)(ESI-)	Eicosanoids, Docosanoids, free FA	45
LC-MS/MS (QToF)(ESI+)	PA, LPA, LPC, LPE, PG, PI, PS, SM, CE, DG, TG	353

Global lipid class composition

It was our aim to investigate the lipid content of the different *S. mansoni* life cycle stages, not restricting our investigation to phospholipids, as done previously [24, 32], but also to include neutral lipids such as sterols, sterol esters and TG. Typical lipidomic profiles (ESI+ mode) obtained for cercariae, worms and eggs are shown in Figure 1. As can be appreciated from Figure 1, PC and TG lipids are the predominantly detected lipid classes. Specifically, we found PC(34:1), PC(36:1), and PC(36:2) to be the major phospholipid species present in all life cycle stages.

The fractional composition shown in Figure 2 indicates that particularly worms and eggs present similar lipid compositions while cercariae have a somewhat different lipid composition. A more detailed depiction comparing the overlapping individual lipid species within different lipid

classes between the distinct life-cycle stages is shown in Figure 3. Interestingly, we could only detect DG lipids in cercariae, but not in the eggs or worms. The same holds true for the species of lysophospholipids (LPC and LPE), which were mainly seen in cercariae and eggs but hardly in worms. On the other hand, there were lower amounts of neutral lipids of the CE and TG type in cercariae. Besides several very common lipids containing oleic or palmitic acid we could also detect some uncommon lipids, such as very long chain LPCs or PCs (i.e. PC(50:6) or LPC(26:2)) (Figure S1). A list of all identified lipids as well as the relative abundance of each lipid species of the total lipid pool from each life cycle stages can be found in supplementary Table S2.

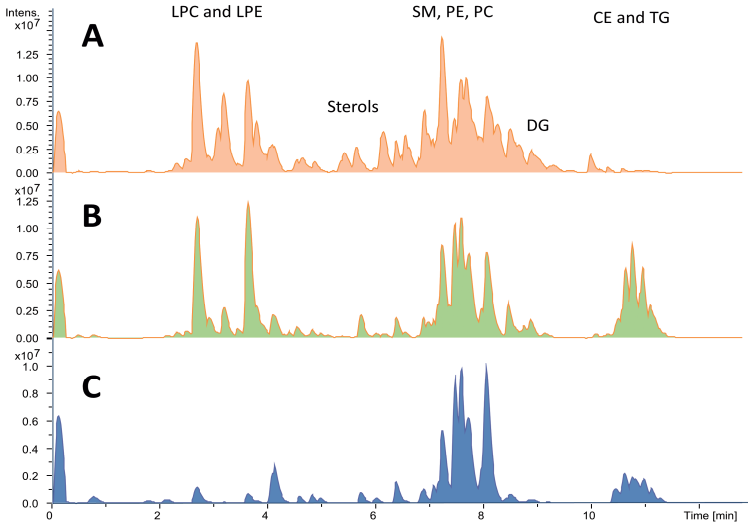

Figure 1. Lipidomic profiles of solid samples (base peak intensity chromatogram)
(A) Cercariae, (B) worms, (C) eggs. LPC (Lyso-Phosphatidylcholine); LPE (Lyso-Phosphatidylethanolamine); SM (Sphingomyelins); PE (Phosphatidylethanolamine); PC (Phosphatidylcholine), CE (Cholesteryl Ester); TG (Triacylglycerol).

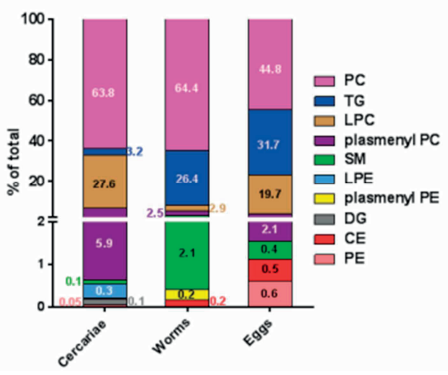

Figure 2. Fractional composition of *S. mansoni* life cycle stages
The percentage (%) fraction of each lipid class is given per life stage. PC (Phosphatidylcholine); TG (Triacylglycerol); LPC (Lyso-Phosphatidylcholine); SM (Sphingomyelins); LPE (Lyso-Phosphatidylethanolamine); DG (Diacylglycerol); CE (Cholesteryl Ester); PE (Phosphatidylethanolamine).

Total fatty acid composition

Next we investigated the total FA composition of the different *S. mansoni* life cycle stages. As can be seen from Table 3 particularly worms contained significant amounts of FA. As expected from the generally low solubility of FA in aqueous media, much lower amounts of FA per µg protein were obtained from AWA and WES.

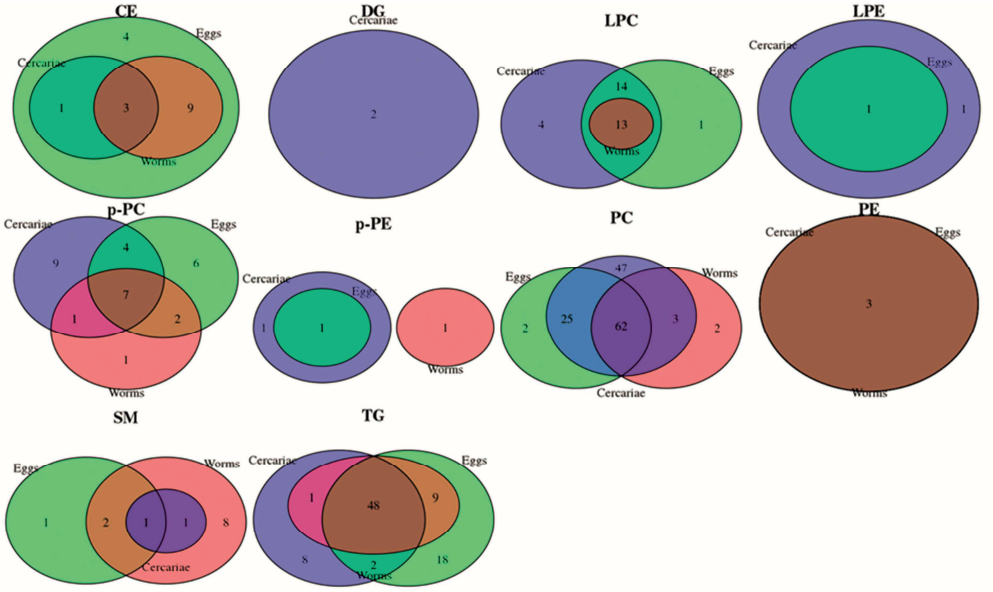

Figure 3. Overlapping lipid species detected in different *S. mansoni* life cycle-stages

CE (Cholesteryl Ester); DG (Diacylglycerol); LPC (Lyso-Phosphatidylcholine); LPE (Lyso-Phosphatidylethanolamine); p-PC (plasmenyl PC); p-PE (plasmenyl-PE); PC (Phosphatidylcholine), PE (Phosphatidylethanolamine), SM (Sphingomyelins), TG (Triacylglycerol).

A

Substance	RRT Standard	RRT Sample
RvE2	0.873	0.870
PDX	0.985	0.984
PD1	0.997	1.000

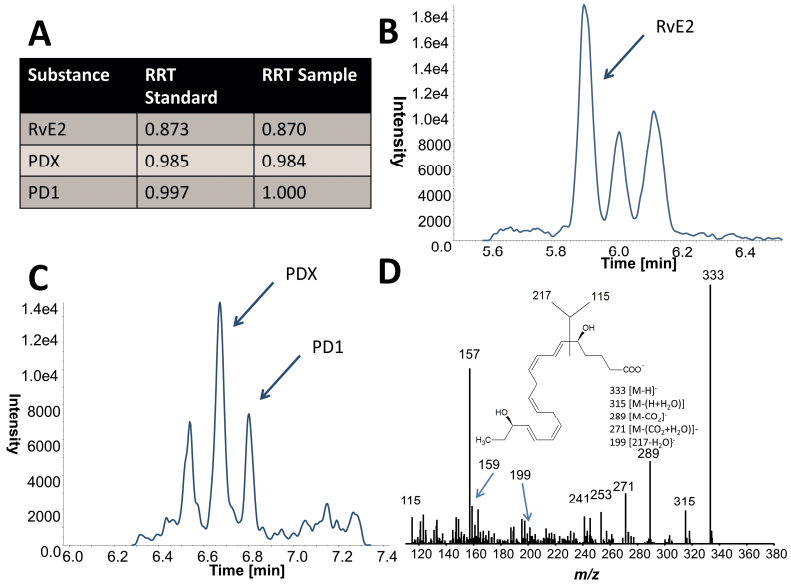

Figure 4. Identification of pro-resolving mediators in cercariae samples

Panel (A) comparison of relative retention times (RRT) between authentic standard material and signals observed in cercariae samples. (B) characteristic extracted ion chromatogram for RvE2 (Resolvin E2). (C) characteristic extracted ion chromatogram for PDX (Protectin DX) and PD1 (Protectin D1). (D) MS/MS spectrum used for the identification of RvE2. The obtained area ratios for PD1 and RvE2 can be found in the supplementary material.

Table 3. A heat-map of total fatty acids composition in ng per µg of protein

Sample type / Analyte	Cercaria	CA	CES	Worms	AWA	WES	Eggs	SEA	EES
FA 10:0	0.0	0.0	0.2	0.2	0.0	0.7	0.0	0.0	0.1
FA 11:0	0.0	0.2	0.8	0.4	0.0	1.9	0.0	0.0	0.5
FA 12:0	0.0	0.2	0.8	0.4	0.0	2.0	0.1	0.0	0.5
FA 13:0	0.0	0.2	0.8	0.4	0.0	1.9	0.0	0.0	0.5
FA 14:0	0.1	0.2	0.9	1.3	0.0	1.9	0.4	0.0	0.5
FA 14:1	0.0	0.2	0.8	0.3	0.0	1.7	0.0	0.0	0.5
FA 15:0	0.1	0.2	0.6	1.6	0.0	1.3	0.7	0.0	0.3
FA 15:1	0.0	0.2	0.6	0.2	0.0	1.3	0.0	0.0	0.3
FA 16:0	2.0	0.3	1.9	80.8	0.1	10.3	38.5	0.2	0.4
FA 16:1	0.1	0.1	0.5	5.0	0.0	0.9	1.4	0.0	0.2
FA 17:0	0.1	0.0	0.0	1.7	0.0	0.1	1.0	0.0	0.0
FA 17:1	0.0	0.0	0.0	0.6	0.0	0.1	0.0	0.0	0.0
FA 18:0	1.8	0.4	3.5	56.7	0.1	14.4	43.5	0.3	0.3
FA 18:1z	2.2	0.1	3.3	141.3	0.2	9.4	39.2	0.2	0.0
FA 18:1e	0.7	0.0	0.3	24.6	0.0	0.9	10.1	0.0	0.0
FA 18:2	3.3	0.1	0.3	100.9	0.1	4.2	70.5	0.3	0.0
FA 18:3 (GLA)	0.0	0.0	0.0	0.3	0.0	0.1	0.4	0.0	0.0
FA 18:3α (ALA)	0.2	0.0	0.1	4.0	0.0	0.2	2.5	0.0	0.0
FA 20:0	0.2	0.0	0.0	2.4	0.0	0.0	1.4	0.0	0.0
FA 20:1	2.0	0.0	0.1	54.1	0.1	6.8	5.0	0.1	0.0
FA 20:2	3.7	0.1	0.1	37.4	0.1	2.1	10.6	0.1	0.0
FA 20:3	0.0	0.0	0.1	6.3	0.0	0.2	1.9	0.0	0.0
FA 20:3α	0.4	0.0	0.3	0.8	0.0	3.1	0.5	0.0	0.1
FA 20:4 (AA)	1.0	0.1	0.6	79.3	0.1	3.7	17.4	0.1	0.2
FA 20:5 (EPA)	1.1	0.1	0.3	0.4	0.0	0.5	0.2	0.0	0.1
FA 22:0	0.1	0.0	0.0	0.5	0.0	0.0	0.2	0.0	0.0
FA 22:1	0.4	0.0	0.2	2.9	0.0	0.3	0.4	0.0	0.1
FA 22:2	0.8	0.0	0.0	2.6	0.0	0.1	0.9	0.0	0.0
FA 22:4 (AdA)	0.3	0.0	0.1	28.3	0.1	2.6	8.5	0.0	0.0
FA 22:5 (DPA)	1.1	0.1	0.4	5.5	0.0	0.8	2.1	0.0	0.1
FA 22:6 (DHA)	0.9	0.1	0.6	8.0	0.0	1.3	5.2	0.0	0.2
FA 24:1	0.1	0.0	0.0	3.2	0.0	0.2	0.3	0.0	0.0

Colour coding based on each parasite material
CA= Cercarial Antigen; CES= Cercarial ES; AWA= Adult Worms Antigen; WES= Worms ES; SEA= Soluble Eggs Antigen; EES= Egg ES

Oxylipid composition

Finally we analyzed the composition of oxylipids of the different life cycle stages and parasite extracts. Table 4 shows that large amounts of Polyunsaturated Fatty Acids (PUFAs) as well as downstream Cyclo-oxygenase (COX) and Lipoxygenase (LOX) derivatives could be detected in several parasite-derived material. Particularly, high levels of PUFA precursors such as Arachidonic Acids (AA), Linoleic Acids (LA) and Docosahexaenoic Acid (DHA) were found in all preparations, relative to their derivatives. Furthermore, the overall composition of COX and LOX derivatives of cercariae and eggs was largely similar but distinct to that of worms. However, an interesting difference between cercariae and eggs was the fact that we could detect several proresolvin lipids, including Protectin D1 (PD1) and (Resolvin E2) RvE2, as LOX derivatives specifically in cercariae, but not in eggs. Figure 4 illustrates the identification of these substances in the investigated samples and demonstrates that our structural assignments were based on several layers of analytical

characteristics. Firstly, we monitored characteristic tandem mass spectrometric transitions (MRM), secondly we compared relative retention times (RRT) with synthetic standard material and lastly we investigated the observed tandem mass spectra for the presence of several substance specific fragment ions.

Table 4. A heat-map of quantified oxylipids in *S. mansoni* preparations in ng per sample

	Sample type / Analyte	Cercaria	CA	CES	Worms	AWA	WES	Eggs	SEA	EES
Tri-hydroxy	LXA_4	0.002	0.000	0.000	0.000	0.000	0.010	0.002	0.030	0.043
	TxB_2	0.000	0.000	0.000	0.000	0.000	0.016	0.000	0.000	0.002
	PGD_2	0.004	0.000	0.000	0.001	0.000	0.012	0.006	0.018	0.029
	PGE_2 (and isomers)	0.018	0.001	0.001	0.012	0.001	0.087	0.019	0.172	0.359
	15-Keto-PGE_2	0.000	0.000	0.000	0.014	0.000	0.007	0.000	0.007	0.019
	8-iso-$PGF_{2\alpha}$	0.002	0.000	0.000	0.000	0.000	0.003	0.003	0.017	0.035
Di-hydroxy	14.15-diHETE	0.037	0.000	0.000	0.000	0.000	0.000	0.060	0.000	0.000
	19.20-DiHDPA	0.009	0.000	0.000	0.001	0.000	0.005	0.013	0.000	0.007
	Leukotriene B_4/5S.12S-diHETE	0.011	0.000	0.000	0.000	0.000	0.000	0.013	0.011	0.000
	6-trans-LTB_4	0.002	0.000	0.000	0.001	0.000	0.001	0.003	0.008	0.000
	PDX	0.019	0.000	0.000	0.000	0.000	0.000	0.025	0.003	0.000
	8S.15S-diHETE	0.017	0.000	0.000	0.000	0.000	0.000	0.021	0.018	0.001
	6t.12epi-LTB_4	0.002	0.000	0.000	0.002	0.000	0.003	0.004	0.012	0.002
	5.15-diHETE	0.040	0.000	0.000	0.000	0.000	0.000	0.051	0.061	0.003
Mono-hydroxy	5-HETE	0.23	0.00	0.01	0.20	0.01	0.05	0.31	0.37	0.01
	8-HETE	0.08	0.00	0.00	0.07	0.00	0.02	0.11	0.30	0.07
	11-HETE	0.13	0.00	0.00	0.05	0.00	0.02	0.16	0.19	0.00
	12-HETE	0.40	0.00	0.00	0.36	0.01	0.10	0.54	0.32	0.01
	15-HETE	0.68	0.00	0.00	0.14	0.01	0.09	0.92	0.54	0.02
	15-HEPE	0.86	0.00	0.00	0.00	0.00	0.00	1.35	0.00	0.00
	18-HEPE	0.80	0.00	0.00	0.00	0.00	0.00	1.09	0.01	0.00
	10-HDHA	0.11	0.00	0.00	0.01	0.00	0.00	0.17	0.07	0.01
	7-HDHA	0.04	0.00	0.00	0.01	0.00	0.01	0.06	0.04	0.00
	17-HDHA	1.18	0.00	0.00	0.03	0.00	0.02	1.89	0.18	0.00
PUFA	AA	638	3.00	8.00	445	15.0	29.0	931	13.0	5.00
	DHA	1586	3.00	7.00	9.03	9.00	8.00	2917	6.00	5.00
	EPA	733	1.00	1.00	5.00	1.00	0.00	1325	1.00	1.00
	AdA	299	1.00	0.00	100	1.00	5.00	499	1.00	0.00
	DPAn-3	573	0.00	0.00	23.0	0.00	2.00	1106	0.00	1.00
	LA	1328	15.0	30.0	357	34.0	53.0	2201	50.0	20.0
	ALA/GLA	128	1.00	1.00	52.0	0.00	3.00	211	2.00	2.00

Colour coding refers to each lipid subclass (mono-, di-, tri-hydroxy, PUFA) per worm preparation/life-stage
CA= Cercarial Antigen; CES= Cercarial ES; AWA= Adult Worms Antigen; WES= Worms ES; SEA= Soluble Eggs Antigen; EES= Egg ES

Conversely, we detected relatively high concentrations of COX products, including prostaglandin D2 (PGD_2) and PGE_2, in eggs and egg-derived antigen preparations. Moreover, apart from PGE_2 itself, several isomers were detected in high amounts in all egg-derived materials. The presence of geometric isomers can hamper substance identification, which is illustrated in Figure 5. When monitoring the PGE_2 characteristic MRM transition *m/z* 351->271 several closely eluting peaks were obtained. Due to the fact that geometric isomers such as the D- and E-series prostaglandins listed in Figure 5 give rise to almost identical tandem mass spectra we had to rely

on RRTs for substance identification. We compared the RRTs with the ones obtained for synthetic standard material as listed in Figure 5, showing the presence of several isomeric prostaglandins particularly present in eggs and egg-derived materials (SEA and EES).

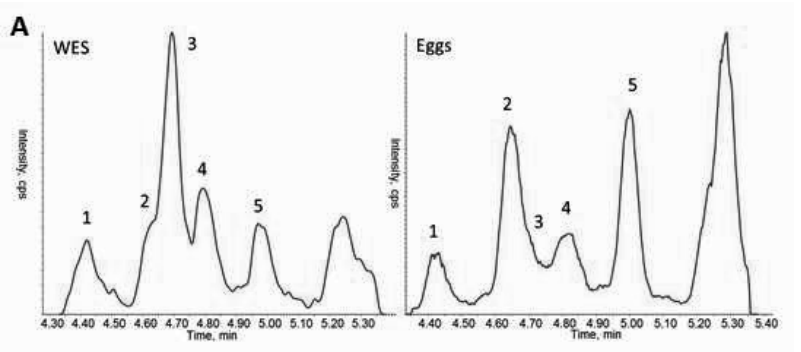

B

Standard	RRT	Compound	RRT	Detected
Δ^{12}-PGD_2	0.943	1	0.944	WES, Eggs
15R-PGE_2	0.947			
8-iso PGE_2	0.957			
15R-PGD_2	0.987	2	0.991	WES, Eggs
PGE_2	1.004	3	1.003	WES, Eggs
15-trans-PGD_2	1.011			
PGD_2	1.023			
11β-PGE_2	1.025	4	1.029	WES, Eggs
15-trans-PGE_2	1.057	5	1.067	WES, Eggs

Figure 5. PGE_2 and Isomer identification with MS/MS trace *m/z* 351 -> 271.

Finally, worms and AWA were found to have a particular enrichment for LTB_4. Although this was also detected in eggs, the signal found in SEA and cercariae could be attributed to isomeric 5S,12S-diHETE, which was revealed by small relative retention time (RRT) differences between the two components, as described by us previously [29, 33]. Concentrations and area ratios of all detected oxylipids can be found in Table 4 and supplementary data (Table S2).

DISCUSSION

In the current study we performed an in-depth lipidomic analysis of the different life cycle stages of *S. mansoni* using three complementary MS-based platforms. In addition, we defined the lipid profile of aqueous extracts from different life stages of *S. mansoni*, which are CA, AWA and SEA, as well as their excretory and secretory products (ES), which are all commonly used antigen preparations in immunoparasitological studies. In total we identified more than 400 lipid species including several bioactive molecules, which we organized in a *S. mansoni* lipid database (supplementary Table S2). For FA, eicosanoids and docosanoids we have generated quantitative data, while a compositional analysis with relative abundances was carried out for higher order lipids. Our data reveal that there are life-stage specific lipid signatures not only for structural lipids but also for bioactive lipid mediators that may be important in host-pathogen interactions.

Global lipid class composition analysis revealed that PC (34:1), PC (36:1), and PC (36:2) are the predominant phospholipid species present in all life cycle stages. In line with this work, Schariter *et al* have described the presence of PC in cercariae [34]. Moreover, our work is also consistent with

earlier work on adult worms by Retra *et al* [23] which also covered phosphoinositol (PI) and phosphatidylserine (PS) lipids and, as such, our work can be seen as complementary to theirs. Earlier work has found that a *S. mansoni*-specific PS fraction conditioned DCs to induce both Th2 and IL-10 producing T cells via TLR2 activation [19]. However, we were unable to detect significant amounts of PS in any of our preparations, this is likely due to the fact that our analytical approach focused on the ESI+ mode to detect PS while Retra *et al.* use the ESI- mode in their study. Furthermore, we observed that global composition of the major lipid classes present in worms and eggs were similar, while cercariae were found to have a distinct profile, with less neutral lipids such as CE and TG. This specific difference is likely to be a direct result of the fact that because *S. mansoni* is unable to synthesize fatty acids and sterols *de novo* [35], it relies on scavenging of lipid precursors from its host to generate complex lipids such as phospholipids and TG [36], a process that free swimming cercariae cannot resort to. In addition our observation that cercariae contain much lower amounts of a large range of free FA we quantified, would support the idea that cercariae, compared to worms and eggs that reside in the host, have limited lipid accessibility.

Oxylipids such as docosanoids and eicosanoids have pleiotropic functions that include shaping the function of immune cells [37]. Hence, mapping and analysis of these known immunomodulatory lipid classes including their precursors was an important part of the present study. We found that cercariae as well as eggs and the antigen preparation derived from these life cycle stages, but less so adult worms, contain significant amounts of PUFAs, such as n3-PUFA (DHA), Eicosapentaenoic Acid (EPA), Docosapentaenoic Acid (DPA) and n6-PUFA (AA), as well as many of their bioactive derivatives that are known to be generated through COX and LOX activity. While cercariae have been shown before to produce various eicosanoids [38], this has not been described for the egg stage. An interesting observation is that despite the absence of COX enzymes in the *S. mansoni* genome [20, 39], we detected various prostaglandins in both cercariae and eggs. This apparent discrepancy has been reported by others as well [40], and it has been postulated that this could be explained by an alternative mechanism for the generation of prostaglandin-like compounds, involving the non-enzymatic generation of molecules called isoprostanes, by auto-oxidation of AA by free-radicals. Indeed, we found evidence for production of isoprostanes in these parasites, which would allow for prostaglandin synthesis in the absence of COX activity. Of the prostaglandins we found PGD_2 and PGE_2 to be the most highly abundant species present in cercariae and eggs. Although PGD_2 may exert pro-inflammatory or anti-inflammatory effects in different biologic systems, in the context of *S. mansoni* it has primarily been linked to limiting the ability of the host to mount a protective immune response against cercariae [41], through its ability to suppress migration of langerhans cells in the skin [18]. Whether PGD_2 produced by eggs has similar immunomodulatory effects remains to be determined. PGE_2, like PGD_2, can have proinflammatory or anti-inflammatory effects depending on the context [42]. One particularly interesting property of PGE_2 is that is has been shown to condition DCs to prime Th2 responses [43]. This property, together with our observation that specifically eggs and SEA, which are well-known for their Th2 polarizing potential, contain high levels of PGE_2, would make it conceivable that PGE_2 contributes to Th2 induction by *S. mansoni* eggs. Further studies would be needed to test this hypothesis.

In addition, we found various potentially immunomodulatory LOX derived products to be present in the different life cycle stages. For instance, in line with other studies [20], the AA-derived LOX product 15-HETE was detected. 15-HETE is known to be a ligand for peroxisome proliferator-activated receptors [44], which when activated in immune cells generally leads to suppression of pro-inflammatory effector responses by these cells. As such, one could speculate that release of

15-HETE by the parasite may locally contribute to suppression of immune responses. Finally, our analyses for the first time reveal that cercariae contain several n3-PUFA derived LOX products including resolvin E2 (RvE2) protectin DX (PDX) and protectin D1 (PD1). These docosanoids are *specialized pro-resolving mediators* that can suppress inflammatory immune responses and are important for promoting resolution of inflammation [45]. Once cercariae have penetrated the skin, they stay in the skin for 3 to 4 days before they enter the circulation. We hypothesize that production of these pro-resolving mediators during this period increases their chances of survival as these factors can suppress recruitment of immune cells and anti-cercariael immune responses. More in depth studies are warranted to further explore the role of resolvin production by *S. mansoni* life cycle stages in host-pathogen interactions and subversion of host immunity.

In conclusion, we have generated a comprehensive dataset defining the lipidome of different life cycle stages of *S. mansoni* in unprecedented detail. Our analysis has revealed several important differences between the lipid composition of the different life cycle stages of *S. mansoni*, that provide new insights into the biology of the parasite itself as well as into how the various life cycle stages interact with and may modulate the host immune system. Moreover, an important observation was that lipid composition of parasite life cycle stages and the corresponding extracts were highly similar, which validates the use of those widely used parasite preparations as models to study host-parasite interactions in immunological studies. Altogether, we believe this work will be a highly useful resource to many researchers in the field of parasitology and immunoparasitology and may serve as a starting point for the identification of immunomodulatory lipids that could be used or targeted, to shape anti-parasite immune responses with regards to vaccination or to develop lipid-based therapeutics to treat inflammatory disorders.

ACKNOWLEDGEMENTS

The authors would like to thank Angela van Diepen, Janneke Kos-van Oosterhoud, Michelle Yang and Marije Kuipers for help with antigens preparations. This work was supported by The Indonesian Directorate General of Higher Education (DGHE/DIKTI)-Leiden University, the company of biologist-Diseases Model and Mechanisms (DMM)-travelling fellowship given to Maria M. M. Kaisar and LUMC fellowship to Bart Everts.

REFERENCES

1. Tomcik, K., et al., *Isotopomer enrichment assay for very short chain fatty acids and its metabolic applications.* Analytical Biochemistry, 2011. **410**(1): p. 110-117.
2. Pearce, E.J. and A.S. MacDonald, *The immunobiology of schistosomiasis.* Nat Rev Immunol, 2002. **2**(7): p. 499-511.
3. Pacifico, L.G., et al., *Schistosoma mansoni antigens modulate experimental allergic asthma in a murine model: a major role for CD4+ CD25+ Foxp3+ T cells independent of interleukin-10.* Infect Immun, 2009. **77**(1): p. 98-107.
4. van der Vlugt, L.E., et al., *Schistosomes induce regulatory features in human and mouse CD1d(hi) B cells: inhibition of allergic inflammation by IL-10 and regulatory T cells.* PLoS One, 2012. **7**(2): p. e30883.
5. Campolina, S.S., et al., *Effective anthelmintic therapy of residents living in endemic area of high prevalence for Hookworm and Schistosoma mansoni infections enhances the levels of allergy risk factor anti-Der p1 IgE.* Results Immunol, 2015. **5**: p. 6-12.
6. Mpairwe, H., et al., *Anthelminthic treatment during pregnancy is associated with increased risk of infantile eczema: randomised-controlled trial results.* Pediatr Allergy Immunol, 2011. **22**(3): p. 305-12.
7. Cardoso, L.S., S.C. Oliveira, and M.I. Araujo, *Schistosoma mansoni antigens as modulators of the allergic inflammatory response in asthma.* Endocr Metab Immune Disord Drug Targets, 2012. **12**(1): p. 24-32.
8. Smits, H.H., et al., *Protective effect of Schistosoma mansoni infection on allergic airway inflammation depends on the intensity and chronicity of infection.* J Allergy Clin Immunol, 2007. **120**(4): p. 932-40.

9. Hasby, E.A., et al., *FoxP3+ T regulatory cells and immunomodulation after Schistosoma mansoni egg antigen immunization in experimental model of inflammatory bowel disease.* Cell Immunol, 2015. **295**(1): p. 67-76.
10. Hussaarts, L., et al., *Chronic helminth infection and helminth-derived egg antigens promote adipose tissue M2 macrophages and improve insulin sensitivity in obese mice.* FASEB J, 2015. **29**(7): p. 3027-39.
11. Neves, L.X., et al., *What's in SWAP? Abundance of the principal constituents in a soluble extract of Schistosoma mansoni revealed by shotgun proteomics.* Parasit Vectors, 2015. **8**: p. 337.
12. Wilson, R.A., *Proteomics at the schistosome-mammalian host interface: any prospects for diagnostics or vaccines?* Parasitology, 2012. **139**(9): p. 1178-94.
13. Jang-Lee, J., et al., *Glycomics analysis of Schistosoma mansoni egg and cercarial secretions.* Mol Cell Proteomics, 2007. **6**(9): p. 1485-99.
14. Smit, C.H., et al., *Glycomic Analysis of Life Stages of the Human Parasite Schistosoma mansoni Reveals Developmental Expression Profiles of Functional and Antigenic Glycan Motifs.* Mol Cell Proteomics, 2015. **14**(7): p. 1750-69.
15. Smith, T.M. and T.J. Brooks, Jr., *Lipid fractions in adult Schistosoma mansoni.* Parasitology, 1969. **59**(2): p. 293-8.
16. Payares, G., et al., *Changes in the surface antigen profile of Schistosoma mansoni during maturation from cercaria to adult worm.* Parasitology, 1985. **91 (Pt 1)**: p. 83-99.
17. Parra, J.F., et al., *Schistosoma mansoni: phospholipid methylation and the escape of schistosomula from in vitro cytotoxic reaction.* Mol Biochem Parasitol, 1986. **21**(2): p. 151-9.
18. Angeli, V., et al., *Role of the parasite-derived prostaglandin D2 in the inhibition of epidermal Langerhans cell migration during schistosomiasis infection.* J Exp Med, 2001. **193**(10): p. 1135-47.
19. van der Kleij, D., et al., *A novel host-parasite lipid cross-talk. Schistosomal lyso-phosphatidylserine activates toll-like receptor 2 and affects immune polarization.* J Biol Chem, 2002. **277**(50): p. 48122-9.
20. Abdel Baset, H., G.P. O'Neill, and A.W. Ford-Hutchinson, *Characterization of arachidonic-acid-metabolizing enzymes in adult Schistisoma mansoni.* Mol Biochem Parasitol, 1995. **73**(1-2): p. 31-41.
21. Furlong, S.T. and J.P. Caulfield, *Schistosoma mansoni: Sterol and phospholipid composition of cercariae, schistosomula, and adults.* Experimental Parasitology, 1988. **65**(2): p. 222-231.
22. Ferreira, M.S., et al., *Screening the life cycle of Schistosoma mansoni using high-resolution mass spectrometry.* Analytica Chimica Acta, 2014. **845**: p. 62-69.
23. Retra, K., et al., *A simple and universal method for the separation and identification of phospholipid molecular species.* Rapid Communications in Mass Spectrometry, 2008. **22**(12): p. 1853-1862.
24. Retra, K., et al., *The tegumental surface membranes of Schistosoma mansoni are enriched in parasite-specific phospholipid species.* Int J Parasitol, 2015. **45**(9-10): p. 629-36.
25. Fahy, E., et al., *Update of the LIPID MAPS comprehensive classification system for lipids.* Journal of Lipid Research, 2009. **50**(Supplement): p. S9-S14.
26. Quehenberger, O., A.M. Armando, and E.A. Dennis, *High sensitivity quantitative lipidomics analysis of fatty acids in biological samples by gas chromatography–mass spectrometry.* Biochimica et Biophysica Acta (BBA) - Molecular and Cell Biology of Lipids, 2011. **1811**(11): p. 648-656.
27. Heemskerk, M.M., et al., *Prolonged niacin treatment leads to increased adipose tissue poly-unsaturated fatty acid synthesis and an anti-inflammatory lipid and oxylipin plasma profile.* Journal of Lipid Research, 2014.
28. Jónasdóttir, H.S., et al., *An Advanced LC–MS/MS Platform for the Analysis of Specialized Pro-Resolving Lipid Mediators.* Chromatographia, 2014. **78**(5-6): p. 391-401.
29. Giera, M., et al., *Lipid and lipid mediator profiling of human synovial fluid in rheumatoid arthritis patients by means of LC–MS/MS.* Biochimica et Biophysica Acta (BBA) - Molecular and Cell Biology of Lipids, 2012. **1821**(11): p. 1415-1424.
30. Jónasdóttir, H.S., et al., *Detection and Structural Elucidation of Esterified Oxylipids in Human Synovial Fluid by Electrospray Ionization-Fourier Transform Ion-Cyclotron Mass Spectrometry and Liquid Chromatography-Ion Trap-MS3: Detection of Esterified Hydroxylated Docosapentaenoic Acid Containing Phospholipids.* Analytical Chemistry, 2013. **85**(12): p. 6003-6010.
31. Kind, T., et al., *LipidBlast in silico tandem mass spectrometry database for lipid identification.* Nat Meth, 2013. **10**(8): p. 755-758.
32. Retra, K., et al., *A simple and universal method for the separation and identification of phospholipid molecular species.* Rapid Commun Mass Spectrom, 2008. **22**(12): p. 1853-62.
33. Jónasdóttir, H.S., et al., *Differential Mobility Separation of Leukotrienes and Protectins.* Analytical Chemistry, 2015. **87**(10): p. 5036-5040.
34. Schariter, J.A., et al., *Determination of neutral lipids and phospholipids in the cercariae of schistosoma mansoni by high performance thin layer chromatography.* J Liq Chrom & Rel Technol, 2002. **25**: p. 1615-22.
35. Meyer, F., H. Meyer, and E. Bueding, *Lipid metabolism in the parasitic and free-living flatworms, Schistosoma mansoni and Dugesia dorotocephala.* Biochim Biophys Acta, 1970. **210**(2): p. 257-66.

36. Brouwers, J.F., et al., *The incorporation, modification and turnover of fatty acids in adult Schistosoma mansoni.* Mol Biochem Parasitol, 1997. **88**(1-2): p. 175-85.
37. Dennis, E.A. and P.C. Norris, *Eicosanoid storm in infection and inflammation.* Nat Rev Immunol, 2015. **15**(8): p. 511-523.
38. Fusco, A.C., B. Salafsky, and M.B. Kevin, *Schistosoma mansoni: eicosanoid production by cercariae.* Exp Parasitol, 1985. **59**(1): p. 44-50.
39. Berriman, M., et al., *The genome of the blood fluke Schistosoma mansoni.* Nature, 2009. **460**(7253): p. 352-8.
40. Noverr, M.C., J.R. Erb-Downward, and G.B. Huffnagle, *Production of eicosanoids and other oxylipins by pathogenic eukaryotic microbes.* Clin Microbiol Rev, 2003. **16**(3): p. 517-33.
41. Abdel-Ghany, R., et al., *Blockade of Pge2, Pgd2 Receptors Confers Protection against Prepatent Schistosomiasis Mansoni in Mice.* J Egypt Soc Parasitol, 2015. **45**(3): p. 511-20.
42. Kalinski, P., *Regulation of immune responses by prostaglandin E2.* J Immunol, 2012. **188**(1): p. 21-8.
43. de Jong, E.C., et al., *Microbial compounds selectively induce Th1 cell-promoting or Th2 cell-promoting dendritic cells in vitro with diverse th cell-polarizing signals.* J Immunol, 2002. **168**(4): p. 1704-9.
44. Naruhn, S., et al., *15-hydroxyeicosatetraenoic acid is a preferential peroxisome proliferator-activated receptor beta/delta agonist.* Mol Pharmacol, 2010. **77**(2): p. 171-84.
45. Serhan, C.N. and N.A. Petasis, *Resolvins and Protectins in Inflammation Resolution.* Chemical Reviews, 2011. **111**(10): p. 5922-5943.

SUPPLEMENTARY DATA

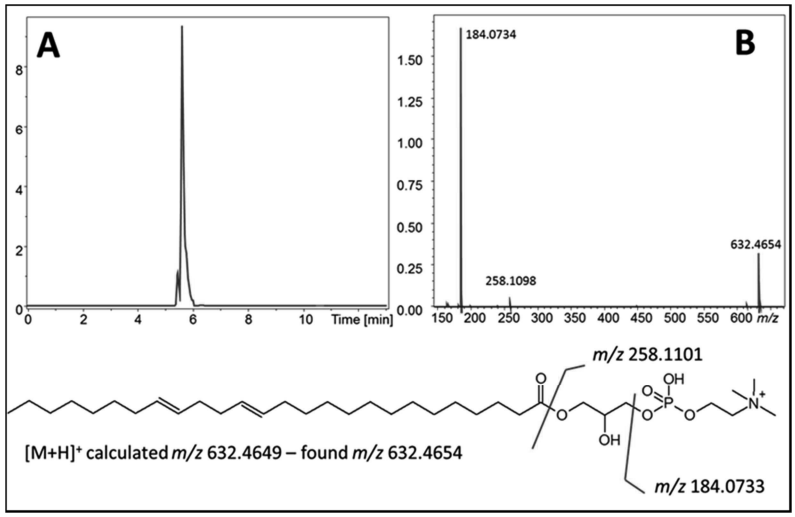

Figure S1. (A) Extracted ionchromatogram of *m/z* 632.465 and (B) Tandem mass spectrum of the very long chain LPC(26:2).

Table S1. A list of monitored oxylipids, corresponding lipidmaps IDs and calibration ranges

Lipid maps ID	Analyte	Calibration line range [ng/mL]
LMFA04000027	10-HDHA	0.025 – 10
LMFA03060085	11-HETE	0.025 – 10
LMFA03060088	12-HETE	0.025 – 10
LMFA02000228	13-HODE	N/A
LMFA02000051	13-HOTrE	N/A
LMFA03060077	14,15-diHETE	0.01 – 2
LMFA03070032	15-HEPE	0.025 – 10
LMFA03060087	15-HETE	0.025 – 10
LMFA04000032	17-HDHA	0.025 – 10
	17-HDoTE	N/A
LMFA03070033	18-HEPE	0.025 – 10
LMFA04000043	19,20-diHDPA	0.01 – 2
LMFA03020018	20-OH-LTB_4	0.01 – 2
LMFA03060084	5-HETE	0.025 – 10
LMFA03020014	6-trans-12-epi-LTB4	0.01 – 2
LMFA03020013	6-trans-LTB_4	0.01 – 2
LMFA04000025	7-HDHA	0.025 – 10
	7S,17S-diHDPA	0.025 – 2
LMFA03060086	8-HETE	0.025 – 10
LMFA03110003	8-iso-PGE_2	0.01 – 2
LMFA03110001	8-iso-$PGF_{2\alpha}$	0.01 – 2
LMFA02000151	9-HODE	N/A
LMFA02000024	9-HOTrE	N/A
LMFA01030001	AA	5 – 500
LMFA01030178	AdA	1 – 200
LMFA01030152	ALA/GLA	N/A
LMFA01030185	DHA	5 – 500
LMFA04000044	DPA_{n-3}	5 – 500
LMFA01030759	EPA	1 – 200
LMFA01030120	LA	5 – 500

Lipid maps ID	Analyte	Calibration line range [ng/mL]
LMFA03020001	LTB_4	0.01 – 2
LMFA03020006	LTD_4	0.01 – 2
LMFA03020002	LTE_4	0.01 – 2
LMFA03010004	PGD_2	0.01 – 2
LMFA03010003	PGE_2	0.01 – 2
LMFA03010002	$PGF_{2\alpha}$	0.025 – 2
LMFA03030002	TXB_2	0.01 – 2
LMFA04000047	10S,17S-diHDHA	0.01 – 2
LMFA03080004	11(12)EET	N/A
LMFA03010031	13,14-dihydro-15-keto-PGE_2	N/A
LMFA03010027	13,14-dihydro-15-keto-$PGF_{2\alpha}$	N/A
LMFA03080005	14(15)EET	N/A
LMFA03010021	15-deoxy-PGJ_2	N/A
LMFA03040010	15-epi-LXA_4	0.01 – 2
LMFA03010030	15-keto-PGE_2	0.01 – 2
LMFA04000074	17-epi-RvD1	N/A
LMFA03070049	18R-RvE3	N/A
LMFA03070048	18S-RvE3	N/A
LMFA03060010	5S,15S-diHETE	N/A
	7-epi-MaR1	N/A
LMFA03080003	8(9) EET	N/A
LMFA03060050	8S,15S-diHETE	0.01 – 2
LMFA03040001	LXA_4	0.01 – 2
LMFA03040002	LXB_4	0.01 – 2
LMFA04000048	MaR1	N/A
LMFA03010019	PGJ_2	N/A
LMFA04000006	RvD1	N/A
LMFA04000007	RvD2	N/A
LMFA03070019	RvE1	N/A
LMFA03070020	RvE2	N/A

Table S2. The relative abundance (%) of each lipid species of the total lipid pool from each life cycle stages of *S. mansoni* and parasites materials derived from *S. mansoni*

Lipid species	Cercariae	CA	CES	Worms	AWA	WES	Eggs	SEA	EES
CE.16.0.				0,01			0,02		
CE.18.0.				0,00			0,05		
CE.18.1.				1,95			0,99		
CE.18.2.	15,27			12,79			6,75	69,20	
CE.18.3.				3,21			2,15		
CE.20.0.							0,00		
CE.20.1.				2,27			3,05		
CE.20.2.				9,77			17,66		
CE.20.3.				3,09			3,44		
CE.20.4.	12,02			17,34			15,21	30,80	
CE.20.5.	19,06						0,65		
CE.22.1.				0,11			0,39		
CE.22.2.							3,16		
CE.22.4.				22,27			16,62		
CE.22.5.	21,41			9,33			7,47		
CE.22.6.	32,24			17,73			22,26		
CE.24.1.				0,12			0,11		
DG.42.3	42,90								
DG.42.4	44,49								
DG.44.3	12,61								
lysoPC.15.0	0,48						0,20		
lysoPC.15.1	0,10								
lysoPC.16.0	21,26		34,66	46,45		36,13	28,79	46,33	
lysoPC.16.1	0,13								
lysoPC.17.0	2,47			1,31			1,30		
lysoPC.17.1	0,15								
lysoPC.17.2	0,04						0,40		
lysoPC.18.0	0,22		49,65	26,18		48,53	0,54	53,67	
lysoPC.18.0.1	12,51						0,29		
lysoPC.18.0.2							32,86		
lysoPC.18.1	3,25		15,69	5,01			6,30		
lysoPC.18.2	1,34						1,67		
lysoPC.18.3	1,98								
lysoPC.20.0	2,08			1,68			2,92		
lysoPC.20.1	8,99			5,63		15,34	8,64		
lysoPC.20.2	11,35			3,25			7,06		
lysoPC.20.3	1,08						0,00		
lysoPC.20.4	0,23						0,77		
lysoPC.20.5	0,23						0,32		
lysoPC.21.0	0,95						0,13		
lysoPC.22.0	1,66			1,25			0,59		
lysoPC.22.1	2,86			0,98			1,08		
lysoPC.22.2	3,51			0,86			1,11		
lysoPC.22.4	0,13						0,45		
lysoPC.22.5	0,19						0,08		
lysoPC.22.6	0,22						0,36		
lysoPC.23.0	1,63			1,49			0,15		
lysoPC.24.0	3,73			3,31			0,80		
lysoPC.24.1	3,79			2,60			0,59		
lysoPC.24.4	0,04						0,13		
lysoPC.25.0	2,78						0,14		
lysoPC.26.0	2,12						0,62		
lysoPC.26.2	3,57						0,59		
lysoPC.O.16.0	4,87						1,12		
lysoPC.P.16.0	0,05								
lysoPE.20.1	33,01								
lysoPE.20.2	51,66								
lysoPE.22.2	15,33								
PC.28.0	0,15								
PC.29.0	0,33								

Lipid species	Cercariae	CA	CES	Worms	AWA	WES	Eggs	SEA	EES
PC.30.0	2,37			0,62			0,37		
PC.30.1	0,37								
PC.31.0	1,74			0,57		1,39	0,56		
PC.31.1	0,56			0,01			0,25		
PC.31.2	0,00			0,18			0,27		
PC.31.3	0,03								
PC.32.0	4,52		14,67	13,76	17,34	36,16	10,14	20,65	
PC.32.1	3,63			1,13			0,95		
PC.32.2	0,25						0,06		
PC.32.3	0,02			0,07					
PC.33.0	0,72			0,31			0,19		
PC.33.1	0,00			0,00			0,00		
PC.33.2	0,39			0,08			0,19		
PC.33.3	0,08			0,16			0,18		
PC.33.4	0,13								
PC.34.0	0,32			3,47	4,54	4,03	2,38		
PC.34.1	6,61		35,39	16,80	21,99	20,61	13,45	24,01	
PC.34.2	0,00			7,84	9,14	5,36	9,52	11,88	
PC.34.3	0,00			0,76			0,97		
PC.34.4	0,25			0,11			0,03		
PC.34.5	0,07								
PC.35.0	0,12			0,21			0,09		
PC.35.1	0,01			0,70			0,51		
PC.35.2	1,34			0,22			0,31		
PC.35.3	0,42						0,06		
PC.35.4	0,12			0,02			0,00		
PC.35.5	0,02			0,06			0,07		
PC.35.6	0,16			0,08			0,05		
PC.36.0	0,10			0,43			0,50		
PC.36.1	8,09		23,15	15,04	20,43	13,22	9,73	13,04	
PC.36.2	0,03		15,04	10,69	14,01	8,02	10,29	12,80	
PC.36.3	0,21			2,51			4,06	5,89	
PC.36.4	2,33			5,99	7,07	3,62	6,70	6,31	
PC.36.5	3,96			0,11			0,25		
PC.36.6	0,00								
PC.37.0	0,06			0,04					
PC.37.1	1,24			0,24			0,27		
PC.37.2	0,45			0,13			0,21		
PC.37.3	0,10			0,06			0,18		
PC.37.4	0,28			0,17			0,19		
PC.37.5	0,00			0,15					
PC.37.6	0,15						0,12		
PC.37.7	0,23								
PC.37.8	0,08								
PC.38.0	0,08			0,08			0,10		
PC.38.1	3,91			1,08		1,31	1,52		
PC.38.2	0,00			1,38		1,51	2,56		
PC.38.3	0,08			1,50			3,09		
PC.38.4	3,70		7,28	3,65	5,48	4,78	4,68	5,42	
PC.38.5	1,61			1,78			2,09		
PC.38.6	1,66			2,20			2,74		
PC.38.7	1,54			0,24			0,06		
PC.38.8	0,05								
PC.39.0	0,05			0,04					
PC.39.1	0,76			0,04			0,04		
PC.39.2	0,84						0,06		
PC.39.3	0,40								
PC.39.4	0,22			0,05			0,03		
PC.39.5	0,27			0,05			0,15		
PC.39.6	0,31			0,00			0,22		
PC.39.7	0,05						0,02		
PC.39.8							0,00		

Lipid species	Cercariae	CA	CES	Worms	AWA	WES	Eggs	SEA	EES
PC.40.0	0,09			0,08			0,07		
PC.40.1	1,82			0,18			0,23		
PC.40.10	0,06								
PC.40.2	3,00			0,19			0,46		
PC.40.3	4,51			0,24			0,82		
PC.40.4	3,58			1,31			0,47		
PC.40.5	1,37			1,07			1,62		
PC.40.6	0,88		4,47	0,51			1,11		
PC.40.7	2,84			0,08			0,32		
PC.40.8	1,52			0,10			0,56		
PC.40.9	0,24			0,04			0,07		
PC.41.0	0,05								
PC.41.1	0,44								
PC.41.2	0,50								
PC.41.3	0,28								
PC.41.4	0,17			0,04			0,05		
PC.41.5	0,12								
PC.41.6	0,18						0,05		
PC.41.7	0,11								
PC.41.8	0,07								
PC.42.0	0,06						0,04		
PC.42.1	0,59			0,06			0,13		
PC.42.10	0,13						0,13		
PC.42.11	0,17						0,00		
PC.42.2	1,72			0,10			0,16		
PC.42.3	2,44			0,08			0,17		
PC.42.4	1,60			0,15			0,32		
PC.42.5	0,79			0,30			0,47		
PC.42.6	1,02			0,30			0,53		
PC.42.7	0,72			0,12			0,07		
PC.42.8	1,70			0,15			0,46		
PC.42.9	0,45						0,09		
PC.43.0	0,02								
PC.43.1	0,20								
PC.43.2	0,28								
PC.43.3	0,19								
PC.43.4	0,06								
PC.43.5	0,06								
PC.43.6	0,08								
PC.44.0	0,02						0,02		
PC.44.1	0,24						0,06		
PC.44.10							0,03		
PC.44.11	0,06						0,01		
PC.44.12	0,05						0,02		
PC.44.2	0,77						0,07		
PC.44.3	1,21						0,07		
PC.44.4	0,39						0,02		
PC.44.5	0,23			0,06			0,14		
PC.44.6	0,60			0,04			0,18		
PC.44.7	0,32						0,03		
PC.44.8	0,26						0,04		
PC.44.9	0,06								
PC.45.1	0,08								
PC.45.2	0,11								
PC.45.3	0,10								
PC.45.4	0,08								
PC.45.5	0,11								
PC.45.6	0,04								
PC.46.1	0,09						0,02		
PC.46.2	0,30						0,04		
PC.46.3	0,44						0,03		
PC.46.4	0,41						0,03		

Lipid species	Cercariae	CA	CES	Worms	AWA	WES	Eggs	SEA	EES
PC.46.5	0,43						0,09		
PC.46.6	0,51						0,07		
PC.46.7	0,28								
PC.46.8	0,07								
PC.47.1	0,02								
PC.47.2	0,04								
PC.47.5	0,04								
PC.47.6	0,04								
PC.48.2	0,10						0,02		
PC.48.3	0,13						0,02		
PC.48.4	0,12						0,02		
PC.48.5	0,15						0,04		
PC.48.6	0,11						0,03		
PC.48.7	0,16								
PC.48.8	0,07								
PC.50.3	0,03								
PC.50.4	0,03								
PC.50.5	0,02						0,02		
PC.50.6	0,02								
PE.38.1							16,26		
PE.38.4							83,74		
PE.40.1	100,00								
plasmenyl.PC.26.0	33,01						12,03		
plasmenyl.PC.27.0	1,33						0,49		
plasmenyl.PC.28.0	5,28						7,25		
plasmenyl.PC.30.0	1,50						2,63		
plasmenyl.PC.30.1							4,41		
plasmenyl.PC.31.0	1,03								
plasmenyl.PC.32.0	3,01			5,47		23,16			
plasmenyl.PC.32.1	0,26								
plasmenyl.PC.33.0	2,52								
plasmenyl.PC.33.1	0,66						0,83		
plasmenyl.PC.33.2				2,59					
plasmenyl.PC.34.0	30,23			44,42		76,84	28,18		
plasmenyl.PC.34.1	0,00			11,30			11,93		
plasmenyl.PC.34.2	1,82			1,05					
plasmenyl.PC.34.3	0,61			1,65			1,86		
plasmenyl.PC.34.4				0,89					
plasmenyl.PC.35.0	2,75			0,61			0,19		
plasmenyl.PC.35.1	1,47			1,24					
plasmenyl.PC.35.2				3,45			0,78		
plasmenyl.PC.36.0	12,59			6,76			5,43		
plasmenyl.PC.36.1	0,00			11,26			11,09		
plasmenyl.PC.36.2	0,00			6,05			5,85		
plasmenyl.PC.36.3				0,67			2,02	100,00	
plasmenyl.PC.37.0	0,26			0,04			0,00		
plasmenyl.PC.37.1	0,19								
plasmenyl.PC.37.2	0,36								
plasmenyl.PC.38.0	1,12			0,77					
plasmenyl.PC.38.4				1,77			3,49		
plasmenyl.PC.42.0							0,30		
plasmenyl.PC.44.0							0,27		
plasmenyl.PC.44.1							0,44		
plasmenyl.PC.46.0							0,28		
plasmenyl.PC.46.1							0,24		
plasmenyl.PE.34.1	100,00								
plasmenyl.PE.36.1				100,00					
SM.33.1				0,87					
SM.34.0				0,89			6,36		
SM.34.1	10,61			51,41		48,77	78,64		
SM.34.2				2,01			1,93		
SM.36.1				5,23		9,62			

Lipid species	Cercariae	CA	CES	Worms	AWA	WES	Eggs	SEA	EES
SM.36.2				2,32					
SM.38.1				3,69		5,89			
SM.38.2				4,80		8,25			
SM.40.1				2,32			1,96		
SM.40.2				14,41		20,94			
SM.41.1				0,55			1,00		
SM.41.5	8,84								
SM.42.1				2,82			2,17		
SM.42.2	43,42			7,07		6,54	7,94		
SM.44.2	37,13			1,60					
TG.46.0							0,08		
TG.46.1							0,08		
TG.48.0				1,24			1,05		
TG.48.1				0,35			0,47		
TG.48.2							0,56		
TG.48.3							0,23		
TG.49.0							0,11		
TG.49.1							0,20		
TG.49.2							0,48		
TG.50.0				1,01			1,17		
TG.50.1	0,58			3,57			5,10	26,09	
TG.50.2	1,34			4,17			10,58	42,01	
TG.50.3				0,78			2,08		
TG.50.4							0,54		
TG.50.5							0,14		
TG.51.0				0,06			0,11		
TG.51.1				0,20			0,38		
TG.51.2	0,69			0,28			0,73		
TG.51.3				0,15			0,32		
TG.51.4							0,28		
TG.52.0				0,27			0,56		
TG.52.1	0,67			2,15			3,86		
TG.52.2	1,87			4,47			8,34	31,90	
TG.52.3	1,85			4,32			6,93		
TG.52.4	1,35			3,43			8,82		
TG.52.5				0,70			2,02		
TG.52.6							0,28		
TG.53.0							0,04		
TG.53.1	0,29			0,10			0,26		
TG.53.2	0,80			0,25			0,52		
TG.53.3	0,84			0,25			0,35		
TG.53.4	0,61			0,18			0,29		
TG.53.5							0,12		
TG.53.6							0,08		
TG.54.0							0,09		
TG.54.1	0,44			0,42			1,20		
TG.54.2	1,94			2,28			3,30		
TG.54.3	4,10			4,43			4,63		
TG.54.4	4,24			5,48			5,42		
TG.54.5	2,27			3,58			3,94		
TG.54.6	1,57			3,58			4,74		
TG.54.7	1,03			0,54			0,79		
TG.54.8							0,09		
TG.55.1	0,16						0,07		
TG.55.2	0,69			0,13			0,19		
TG.55.3	1,31			0,22			0,21		
TG.55.4	1,27			0,18			0,16		
TG.55.5	0,70			0,14					
TG.55.6	0,47			0,13			0,08		
TG.55.7	0,33								
TG.56.1	0,15			0,06			0,17		
TG.56.2	1,06			0,62			0,72		

Lipid species	Cercariae	CA	CES	Worms	AWA	WES	Eggs	SEA	EES
TG.56.3	3,24			2,57			1,31		
TG.56.4	4,44			4,23			1,91		
TG.56.5	4,08			4,61			1,86		
TG.56.6	3,34			5,40			2,02		
TG.56.7	2,28			5,54			1,40		
TG.56.8	1,44			2,96			2,05		
TG.56.9	0,75			0,23			0,27		
TG.57.2	0,33						0,05		
TG.57.3	0,85			0,11			0,07		
TG.57.4	1,01			0,12					
TG.57.5	0,70								
TG.57.6	0,54			0,12					
TG.58.1							0,05		
TG.58.10	1,10			2,35			0,63		
TG.58.11	0,70			0,05			0,07		
TG.58.12	0,35								
TG.58.2	0,36			0,18			0,15		
TG.58.3	1,53			0,89			0,33		
TG.58.4	3,56			1,62			0,48		
TG.58.5	5,02			1,90			0,56		
TG.58.6	4,71			2,62			0,56		
TG.58.7	3,68			3,43			0,49		
TG.58.8	3,27			2,70			0,65		
TG.58.9	2,24			3,18			0,51		
TG.59.2	0,10								
TG.59.3	0,31								
TG.59.4	0,44								
TG.59.5	0,38								
TG.60.10	1,34			0,82			0,20		
TG.60.11	0,87			0,29			0,16		
TG.60.12	0,67			0,41			0,19		
TG.60.13	0,35								
TG.60.2	0,09			0,04			0,06		
TG.60.3	0,46			0,19			0,12		
TG.60.4	1,35			0,38			0,14		
TG.60.5	2,22			0,46			0,14		
TG.60.6	2,27			0,63			0,14		
TG.60.7	1,96			0,72			0,13		
TG.60.8	2,16			0,59			0,16		
TG.60.9	1,90			0,80			0,13		
TG.62.11	0,40								
TG.62.12	0,32			0,11			0,06		
TG.62.13	0,24								
TG.62.14							0,05		

Table S3. The ratio of detected oxylipids from each life cycle stages of *S. mansoni* and parasites materials derived from *S. mansoni*

Oxylipid	Cercariae	CA	CES	Worms	AWA	WES	Eggs	SEA	EES
LXA4	0,01					0,04	0,57	0,08	0,11
5-HETE	0,67	0,01	0,01	0,42	0,02	0,11	10,79	0,79	0,03
8-HETE	0,29			0,18	0,01	0,04	4,12	0,81	0,27
11-HETE	2,03	0,01	0,01	0,62	0,04	0,24	23,80	2,33	0,06
12-HETE	1,75	0,01	0,04	1,18	0,04	0,31	20,17	1,05	0,02
15-HETE	3,32		0,04	0,51	0,05	0,32	41,46	1,95	0,08
15-HEPE	4,00				0,00		0,36		
18-HEPE	3,09	0,01		0,01		0,01	0,45	0,01	
LXB4									
Leukotriene B4	0,04						0,18	0,04	
17-HDHA	1,58		0,01	0,02		0,02	9,14	0,22	
14,15-diHETE	0,05								
19,20-DiHDPA	0,05			0,01		0,02	2,37		0,04
RvE1							0,04		
RvE2	0,10								
18S-RvE3									
18R-RvE3									
TxB2						0,08	0,04		0,03
6-trans-LTB4	0,01			0,00		0,01	0,14	0,02	
20-OH LTB4									
PGD2	0,04			0,01		0,07	0,93	0,10	0,17
PDX	0,06						0,01	0,01	
PD1	0,03							0,01	
MaR1_2									
AT-LXA4									
LTE4							0,03		
8S,15S-diHETE	0,02							0,02	0,00
LTD4									
Leukotriene B4 d4									
15-HETE d8									
PGE2-d4									
7,17-DiHDPA									
RvD1									
RvD2									
6t,12epi-LTB4	0,01	0,00		0,00		0,01	0,08	0,04	0,01
PGF2a				0,01	0,47		0,48		0,09
PGE2_2	0,27	0,03	0,03	0,18	0,03	1,19	16,90	2,33	4,87
17-OH-DH-HETE	0,54	0,01	0,01	0,15		0,06	6,14	0,57	0,01
13-HoTrE	0,77					0,01	0,42	0,08	
13-HoDE	30,60	0,31	0,33	0,91	0,41	0,67	65,06	16,18	0,75
7S-MaR1									
AT-RvD1	0,00	0,00	0,00	0,00	0,00	0,00	0,05	0,00	0,00
15-Keto-PGE2				0,07		0,03	0,80	0,03	0,10
13,14dihydro-15keto-PGE2	0,00	0,00	0,00	0,00	0,00	0,03	0,11	0,02	0,11
13,14dihydro-15keto-PGF2a									
8-iso-PGE2									
8-iso-PGF2a	0,01					0,01	0,50	0,04	0,09
9-HoTrE	0,37	0,01	0,01	0,03	0,01	0,02	1,41	0,15	0,02
9-HoDE	7,84	0,29	0,26	0,85	0,33	0,46	34,44	10,50	0,95
AA	8,37	0,04	0,08	4,00	0,14	0,27	44,79	0,12	0,06
DHA	51,68	0,06	0,13	1,66	0,16	0,14	135,66	0,12	0,09
EPA	37,45	0,02	0,04	0,13	0,04	0,01	10,14	0,04	0,02
AdA	5,43	0,01	0,01	1,08	0,01	0,06	67,85	0,01	0,01
DPAn-3	17,33	0,00	0,02	0,36	0,01	0,02	39,81	0,01	0,01
DHAd5									
LA	6,91	0,06	0,11	1,13	0,12	0,18	23,66	0,17	0,08

Oxylipid	Cercariae	CA	CES	Worms	AWA	WES	Eggs	SEA	EES
ALA	1,81	0,01	0,02	0,51	0,03	0,03	31,85	0,03	0,02
PGJ2	0,07								
5,15-diHETE	0,09						0,09	0,11	0,02
10-HDHA	0,50			0,03		0,01	3,11	0,19	0,02
7-HDHA	0,08			0,01		0,01	0,67	0,07	
5F3T IsoP	0,01	0,00	0,00	0,00	0,00	0,00	0,00	0,00	0,00
14(15)EET	0,11	0,03	0,02	0,41	0,03	0,03	3,04	0,04	0,02
11(12)EET	0,13	0,04	0,04	0,88	0,04	0,06	6,40	0,05	0,05
8(9)EET	0,04		0,02	0,34	0,02	0,02	2,41		0,03
15Deoxy PGJ2							0,08		
4F4T NP	0,03	0,00	0,00	0,00	0,00	0,00	0,61	0,02	0,03
17F2 Dihomo IsoP	0,02	0,00	0,00	0,00	0,00	0,03	1,82	0,15	0,17
10S17R-diHAdA									
ALA_2	0,30	0,00	0,00	0,08		0,01	3,01	0,00	0,00
GLA	0,32	0,00	0,00	0,09	0,01	0,01	6,04	0,01	0,00
4-HDHA	0,46		0,01	0,04		0,01	5,21	0,15	0,01
12-HEPE	2,13			0,02		0,01	0,30		
5-HEPE	1,22		0,00			0,00	0,15	0,01	
14(S)-HDHA	0,94		0,01	0,19		0,02	7,43	0,21	0,01
12-KETE	0,03			0,04			0,98		
DGLA	4,75		0,01	0,33		0,01	17,78	0,02	
5-KETE	0,05		0,03	0,54		0,04	13,30	0,12	
DPAn-6	11,58	0,01	0,01	0,80	0,01	0,04	132,75	0,01	0,01
19(20)EpDPA	0,32			0,07		0,02	6,33	0,08	
15-KETE	0,05		0,02	0,67	0,03	0,06	19,00	0,30	0,05
20-HETE_2	0,03			0,01			0,73		
20-HETE									